nature materials

SUPPLEMENTARY INFORMATION

https://doi.org/10.1038/s41563-019-0356-x

In the format provided by the authors and unedited.

In situ probing electrified interfacial water structures at atomically flat surfaces

Chao-Yu Li[1,3], Jia-Bo Le[1,3], Yao-Hui Wang[1], Shu Chen[2], Zhi-Lin Yang[2], Jian-Feng Li[1,2*], Jun Cheng[1*] and Zhong-Qun Tian[1]

[1]State Key Laboratory of Physical Chemistry of Solid Surfaces, Collaborative Innovation Center of Chemistry for Energy Materials (iChEM), MOE Key Laboratory of Spectrochemical Analysis and Instrumentation, College of Chemistry and Chemical Engineering, Xiamen University, Xiamen, China. [2]Department of Physics, Xiamen University, Xiamen, China. [3]These authors contributed equally: Chao-Yu Li, Jia-Bo Le *e-mail: li@xmu.edu.cn; chengjun@xmu.edu.cn

Supplementary Information for

In situ probing electrified interfacial water structures at atomically flat surfaces

Chao-Yu Li[1,3], Jia-Bo Le[1,3], Yao-Hui Wang[1], Shu Chen[2], Zhi-Lin Yang[2], Jian-Feng Li[1,2]*, Jun Cheng[1]* & Zhong-Qun Tian[1]

[1]State Key Laboratory of Physical Chemistry of Solid Surfaces, Collaborative Innovation Center of Chemistry for Energy Materials (iChEM), MOE Key Laboratory of Spectrochemical Analysis and Instrumentation, College of Chemistry and Chemical Engineering, Xiamen University, Xiamen, China.

[2]Department of Physics, Xiamen University, Xiamen, China.

[3]These authors contributed equally to this work.

Table of contents

Materials and Methods

Preparation of Au SHINs

At first, 55-nm Au core nanospheres were prepared according to the reference[1]: 1.4 mL of sodium citrate solution (1 wt%) was added into 200 mL of boiling $HAuCl_4$ solution (0.01 wt%). And then, the mixture was refluxed for about 1 h. The Au SHINs were prepared according to the reference[2]: 0.4 mL of (3-aminopropyl) trimethoxysilane (APTMS) solution (1 mM) was mixed with 30 mL of the as-prepared Au sol, and then 3.2 mL of sodium silicate solution (0.54 wt%) with a pH of ~10 was added to the sol. Next, the sol was transferred to 95 °C bath and stirred for about 30 min for the coating of 2-nm silica shell. The as-prepared SHINs were centrifuged twice and washed by ultra-pure water. Then, the concentrated sol was diluted with ultra-pure water in the following in situ electrochemical Raman experiments.

Preparation of Au single crystal electrodes and electrochemical Raman measurements

The Au single crystal electrodes were Clavilier-type half-bead single crystal electrodes. Unreconstructed and island-free Au(111)-(1×1) and Au(100)-(1×1) electrodes were prepared according to the reference[3]. Briefly, the Au electrodes were annealed with a butane flame for 2 min and cooled down in an argon atmosphere. Then, the electrodes were immersed into HCl solution (10 mM) at open circuit conditions for ~10 min to lift the reconstruction. The electrodes were extensively rinsed with ultra-pure water to remove the Cl^- ions. Finally, the Au single crystal electrodes were dried in argon stream. Diluted Au SHINs sol was drop-casted onto the freshly prepared Au single crystal electrode surface and then dried under a vacuum condition. And then a HER cleaning procedure has been carried out. To remove the possible contamination, the modified electrodes were cleaned using extensive hydrogen evolution reaction (HER) according to the reference[4]. The electrode was mounted into a vertically oriented electrochemical cell and added with 0.1 M $NaClO_4$ as electrolyte. A potential of −2.0 V vs. Ag/AgCl was applied for HER procedure. Each HER cleaning lasts ~50 seconds and then rinsing the electrode surface with ultrapure water, that procedure was repeated by 3~4 times[4]. The electrode was then immersed in HCl solution (10 mM) for ~10 min to lift the reconstruction, and then rinsed extensively using water again. As systematically discussed in literature, HER cleaning procedure

is effective and nondestructive for Au single crystal surfaces[4]. A home-made spectroelectrochemical cell was used for the *in situ* electrochemical Raman measurements, where a Pt wire and an Ag/AgCl electrode were used as counter and reference electrode. During the electrochemical Raman, the potential was scanned from the negative (-2.0 V vs. Ag/AgCl) toward the positive with an interval of 0.2 V. The PZC at 0.29 and 0.13 V vs. Ag/AgCl is used as the potential references for Au(111) and Au(100) electrodes, respectively[5]. To effectively avoid the interference from hydrogen bubbles on the electrode surface at very negative potentials, we used a thin-layer cell configuration[4,6]. As a result, the gas was quickly dispersed in very fine bubbles, and then escaped smoothly.

Computational models

The Au(111) surface was modeled by a $p(4 \times 4)$ periodic supercell slab with 6 atomic layers. The vacuum space between the slab and its periodic image is 21 Å, and the size of Au(111) supercell is $11.738 \times 11.738 \times 32.98$ Å^3. The lattice constant of Au was optimized by a $6 \times 6 \times 6$ bulk model, containing 864 atoms in total. The calculated lattice constant of Au is 4.15 Å, is in good agreement with the experimental value (4.08 Å). The work function of the Au(111) surface was calculated, and the value of 5.2 eV is very close to the experimental result of 5.3 eV[7]. The Au(111)-water interfaces were modelled by fully filling the vacuum space between the Au slabs with water molecules, keeping the density of water in the bulk 1 g/mL. The model of the Au(111)-water interface overall contains 96 metal atoms and 69 H_2O molecules, consisting of two symmetric interfaces. The water molecules in the interfaces were pre-equilibrated with classical molecular dynamics (MD) simulations for ~100 ps. When there is no net charge pre-set on the metal surface, the condition of the Au(111)-water interface corresponds to the potential of zero charge (PZC) in electrochemistry and its structure has been reported recently[8].

The electric double layers (EDLs) at Au(111)-water interfaces were constructed by inserting Na ions at ~3 Å (Stern layer) away from the Au surface, and the ionic nature of Na^+ is evidenced by the structure of its first hydration layer. Since the model is kept charge neutral, the same number of electrons as that of Na^+ will simultaneously go to the Fermi level of the metal surface, forming an electric double layer (EDL). In our EDL model, the surface charge density is controlled by varying the number of Na^+ included. Note that the charge composition of

electrolyte solution is inevitably changed in our model at different voltage conditions and co-ions (i.e. anions at negatively charged surfaces) are omitted due to the limited size of our DFTMD cell. A consequence is that the charges in EDL are disconnected with those in bulk electrolyte solution, and thus the thermodynamics of Gibbs adsorption isotherm is missing. This however should be of little concern for the application to the potential difference and water structure in EDL in this work owing to the following reasons: Firstly, the potential difference in EDL is determined by the charge excess, instead of the total charge concentrations including both counter-ions and co-ions. Our present EDL model has the correct charge excess by construction. Secondly, in the timescale of DFTMD, the counter-ions in EDL stay in the compact layer not diffusing away from the surface, and the equilibrium between ions in EDL and in bulk electrolyte solution is not reached. Thus, the EDL model closely resembles the compact Helmholtz layer at the high ionic strength limit when the Gouy-Chapman layer is effectively suppressed. This EDL model has been successfully applied to the TiO_2 water interface, and indeed reasonably reproduced the EDL capacitance[9].

We modeled a series of Au(111) EDLs with the Na^+ number ranging from 2 to 10 with an interval of 2, i.e. 1 to 5 per surface (two symmetric interfaces in our models), and the corresponding surface charge densities are –13.4, –26.8, –40.2, –53.6 and –67 $\mu C/cm^2$. The electrode potentials corresponding to different charge densities were calculated by using a recently developed computational standard hydrogen electrode method[10]. The calculated PZC of Au(111) of the $p(4 \times 4)$ cell is 0 V *vs* SHE, differing by ~0.5 V from the experimental value [5]. This discrepancy can be attributed to by the finite size effect on the Fermi level of the metal surface because our recent study using a larger $p(6 \times 6)$ surface shows the PZC can be accurately obtained [10]. We expect that this finite size error is the same for all our EDL models, and can be effectively cancelled when relative values are used. Thus, we have referenced all the calculated electrode potentials to the PZC of Au(111) when comparing with experimental results.

Calculation methodology

The density functional theory (DFT) implementation in CP2K/Quickstep[11] is based on a hybrid Gaussian plane wave (GPW) scheme, the orbitals are described by an atom centered Gaussian-type basis set, and an auxiliary plane wave basis set is used to re-expand the electron

density in the reciprocal space. A matrix diagonalization procedure was used for the wave function optimization and the self-consistent field (SCF) convergence was facilitated by Fermi smearing with the electronic temperature of 300 K. The 2s, 2p electrons of O, 2s, 2p, 3s electrons of Na and 5d, 6s electrons of Au were treated as valence, and the rest core electrons were represented by Goedecker-Teter-Hutter (GTH) pseudopotentials[12,13]. The Gaussian basis set was double-ς with one set of polarisation functions (DZVP)[14], and the plane wave cutoff was set to 400 Ry. Perdew-Burke-Ernzerhof (PBE) functional[15] was used to describe the exchange-correlation effects, and the dispersion correction was applied in all calculations with the Grimme D3 method [16]. In static calculations, the geometries were optimized by Broyden-Fletcher-Goldfarb-Shanno (BFGS) minimizer. For sampling the structures of the interface models and bulk solution, Born-Oppenheimer molecular dynamics (BOMD) was employed, and canonical ensemble (NVT) conditions were imposed by a Nose-Hoover thermostat with a target temperature of 330 K. The MD time step is set to 0.5 fs. For all the MD trajectories, the initial ~3 ps (6000 steps) was regarded as the equilibration period, and then followed by production periods of more than 10 ps. Note that due to the large size of the supercells, only Γ point was used in all calculations. The velocity density of states of interfacial water (within 6 Å from the Au surface) were calculated by the Fourier transformation of the H-H velocity-velocity autocorrelation functions in the DFTMD trajectories.

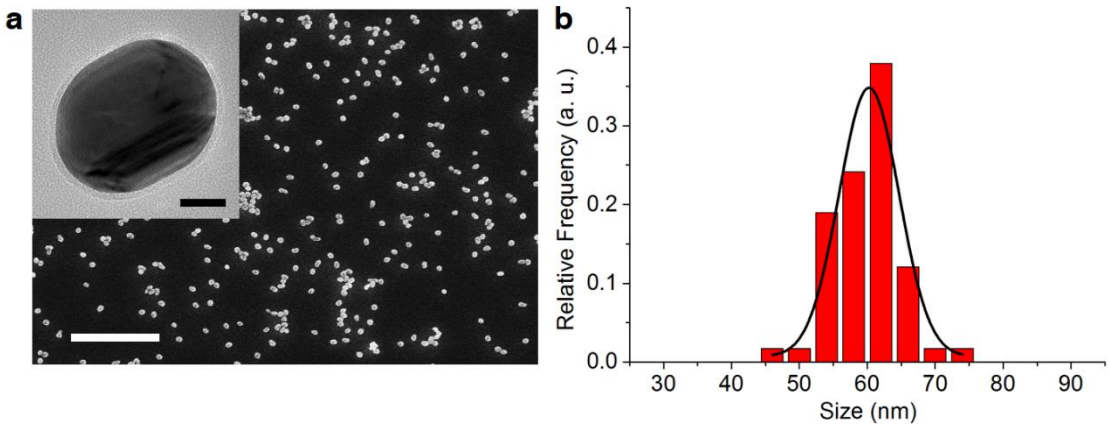

Supplementary Figure 1. (**a**) SEM image of Au(111) surface modified with a sub-monolayer of Au SHINs, where scale bar is 1 μm. The inset shows the high-resolution TEM image of a single Au SHIN, and the scale bar is 20 nm. (**b**) Size distribution of Au SHINs.

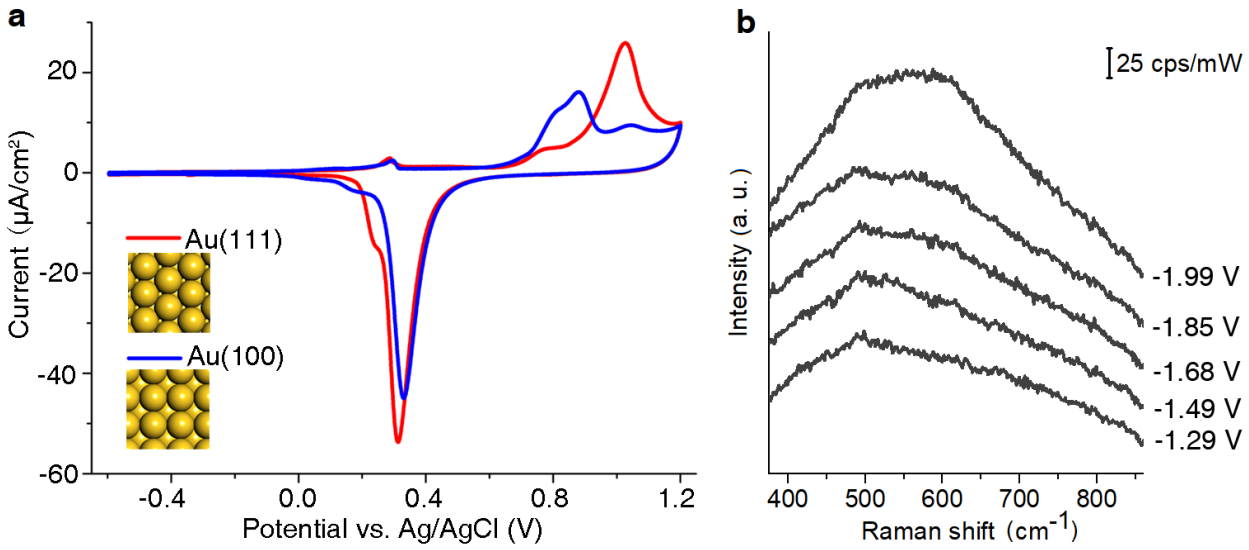

Supplementary Figure 2. (**a**) CVs of Au(111) and Au(100) electrodes in 0.1 M Na_2SO_4 solution, where the scan rate is 10 mV/s and the insets present the atomic models of Au(111) and Au(100) surfaces. The potential is referred to Ag/AgCl electrode; (**b**) In situ potential-dependent Raman spectra of libration modes of interfacial water on Au(111) electrode surface in 0.1 M Na_2SO_4 solution, and the potential is referred to PZC.

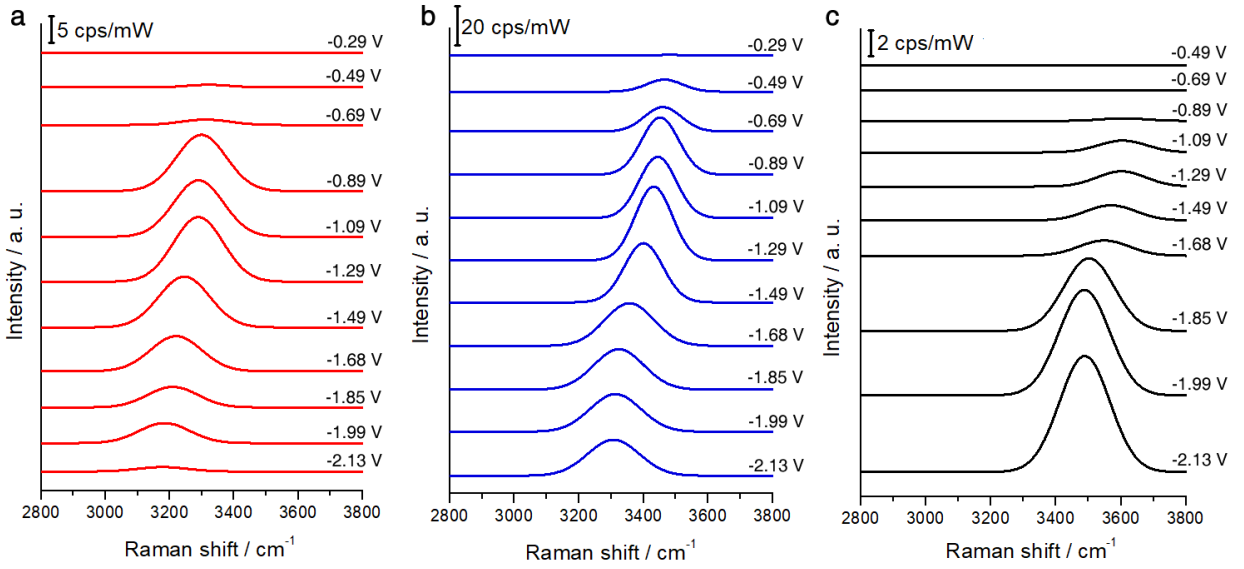

Supplementary Figure 3. Fitted electrochemical Raman spectra of the O-H stretching mode ($\nu_{O\text{-}H}$) of interfacial water at the Au(111) surface measured in 0.1 M Na_2SO_4 solution. (**a**), (**b**) and (**c**) correspond to the fitted Raman peaks with the small, medium, and large wavenumber shown in Fig. 2a, respectively. The scale bars in (a), (b) and (c) are 5, 20 and 2 cps/mW, respectively.

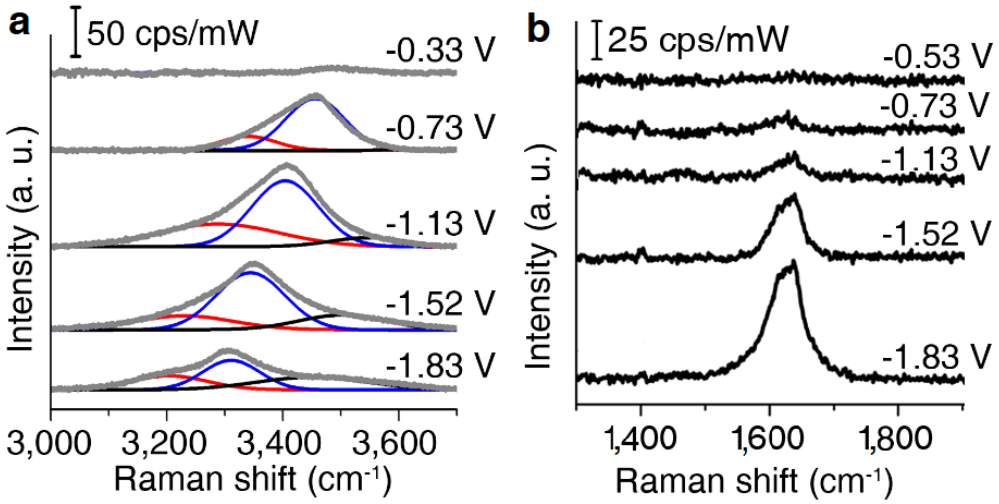

Supplementary Figure 4. In situ electrochemical Raman spectra of O-H stretching mode (**a**) and H-O-H bending mode (**b**) of interfacial water at Au(100) surface in 0.1 M Na_2SO_4 solution. The potentials are referred to PZC.

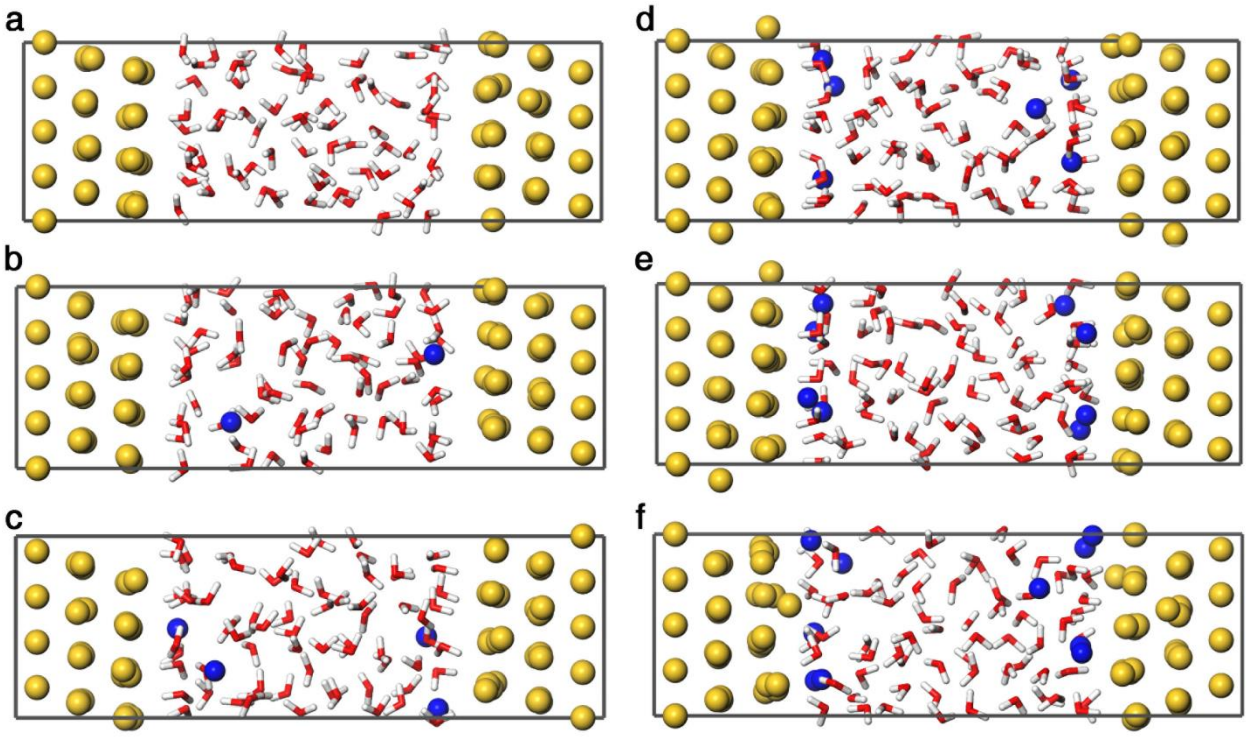

Supplementary Figure 5. AIMD models of the EDLs at the Au(111) surface, where Au and Na atoms are colored by yellow and blue, respectively, and water molecules are represented by the stick model. (**a**)-(**f**) correspond to the potential conditions at 0, -0.19, -0.84, -1.34, -1.89 and -2.16 V with reference to the PZC, respectively.

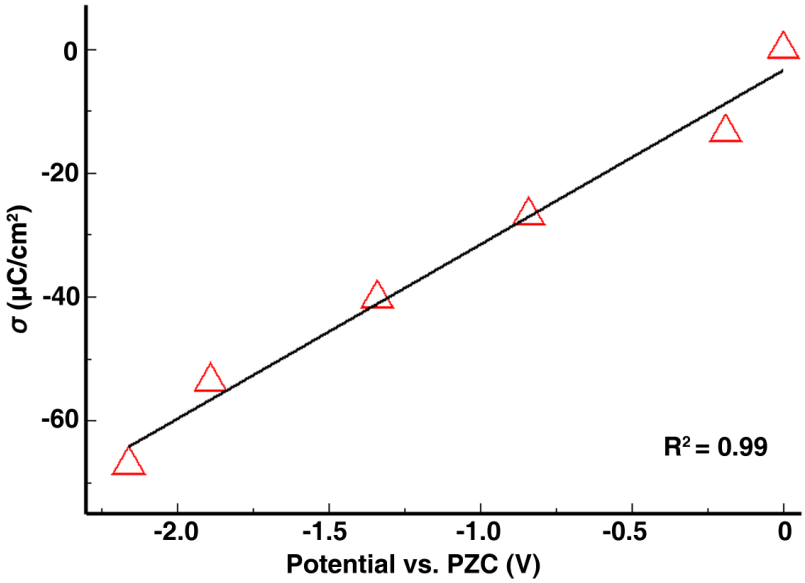

Supplementary Figure 6. Calculated charging curve at the Au(111)/water interfaces. The surface charge densities (σ) are controlled by the number of Na^+ ions included in the electric double layer models, while the corresponding electrode potentials are calculated using the DFTMD method. All the potentials are referenced to the PZC of the Au(111)/water interface. The trend line in black is the linear fit of the calculated data points (red triangle), and the slope indicates the double layer capacitance of ~30 μF/cm^2.

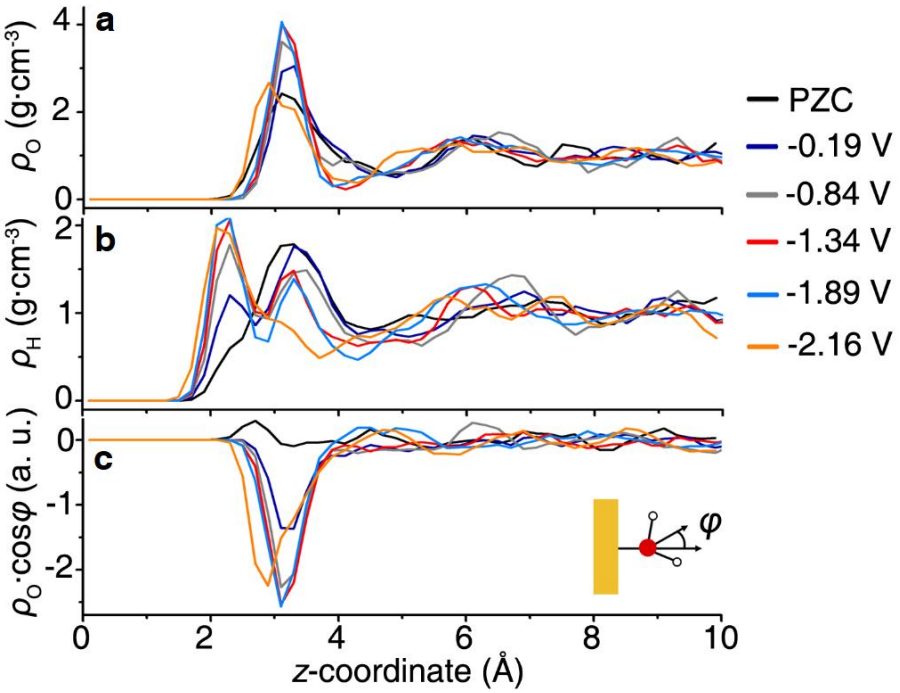

Supplementary Figure 7. Oxygen density (**a**), hydrogen density (**b**), and water dipole-orientation (**c**) distributions along the surface normal (average of the two symmetric interfaces in our models). The coordinate zero corresponds to the position of the metal surface. The inset in (c) illustrates the angle φ between the water bisector and the surface normal.

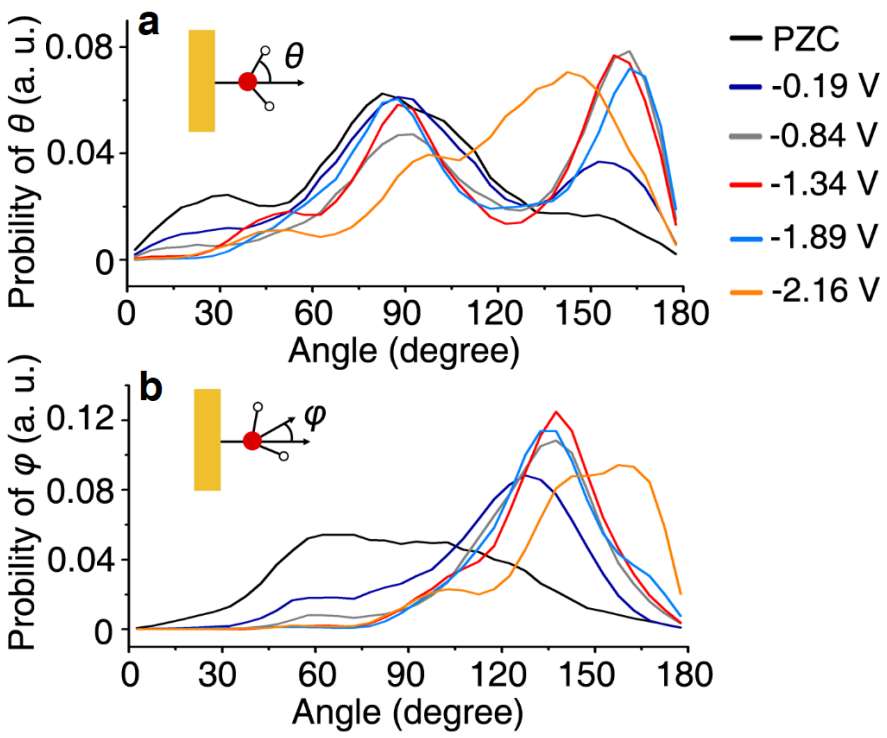

Supplementary Figure 8. Probability distribution functions of the angle θ between the O-H bond and the surface normal (**a)** and the angle φ between the water bisector and the surface normal (**b)** of the interfacial water.

References

1 Frens, G. Controlled nucleation for the regulation of the particle size in monodisperse gold suspensions. *Nature Phys. Sci.* **241**, 20-22, (1973).

2 Li, J. F. *et al.* Shell-isolated nanoparticle-enhanced Raman spectroscopy. *Nature* **464**, 392-395, (2010).

3 Hölzle, M. H., Wandlowski, T. & Kolb, D. M. Phase transition in uracil adlayers on electrochemically prepared island-free Au(100)−(1 × 1). *J. Electroanal. Chem.* **394**, 271-275, (1995).

4 Li, J. F., Rudnev, A., Fu, Y., Bodappa, N. & Wandlowski, T. *In situ* SHINERS at electrochemical single-crystal electrode/electrolyte interfaces: tuning preparation strategies and selected applications. *ACS Nano* **7**, 8940-8950, (2013).

5 Kolb, D. M. & Schneider, J. Surface reconstruction in electrochemistry: Au(100-(5 × 20), Au(111)-(1 × 23) and Au(110)-(1 × 2). *Electrochim. Acta* **31**, 929-936, (1986).

6 Tian, Z. Q. & Ren, B. Adsorption and reaction at electrochemical interfaces as probed by surface-enhanced Raman spectroscopy. *Annu. Rev. Phys. Chem* **55**, 197–229, (2004).

7 Michaelson, H. B. The work function of the elements and its periodicity. *J. Appl. Phys.* **48**, 4729-4733, (1977).

8 Le, J., Cuesta, A. & Cheng, J. The structure of metal-water interface at the potential of zero charge from density functional theory-based molecular dynamics. *J. Electroanal. Chem.* **819**, 87-94, (2018).

9 Cheng, J. & Sprik, M. The electric double layer at a rutile TiO_2 water interface modelled using density functional theory based molecular dynamics simulation. *J. Phys. Condens. Matter* **26**, 244108, (2014).

10 Le, J., Iannuzzi, M., Cuesta, A. & Cheng, J. Determining potentials of zero charge of metal electrodes versus the standard hydrogen electrode from density-functional-theory-based molecular dynamics. *Phys. Rev. Lett.* **119**, 016801, (2017).

11 VandeVondele, J. *et al.* Quickstep: Fast and accurate density functional calculations using a mixed Gaussian and plane waves approach. *Comput. Phys. Commun.* **167**, 103-128, (2005).

12 Goedecker, S., Teter, M. & Hutter, J. Separable dual-space Gaussian pseudopotentials. *Phys. Rev. B* **54**, 1703-1710, (1996).

13 Hartwigsen, C., Goedecker, S. & Hutter, J. Relativistic separable dual-space Gaussian pseudopotentials from H to Rn. *Phys. Rev. B* **58**, 3641-3662, (1998).

14 Vandevondele, J. & Hutter, J. Gaussian basis sets for accurate calculations on molecular systems in gas and condensed phases. *J. Chem. Phys.* **127**, 114105, (2007).

15 Perdew, J. P., Burke, K. & Ernzerhof, M. Generalized gradient approximation made simple. *Phys. Rev. Lett.* **77**, 3865-3868, (1996).

16 Grimme, S., Antony, J., Ehrlich, S. & Krieg, H. A consistent and accurate *ab initio* parametrization of density functional dispersion correction (DFT-D) for the 94 elements H-Pu. *J. Chem. Phys.* **132**, 154104, (2010).